JOURNAL OF GEOPHYSICAL RESEARCH, VOL. 114, C07027, doi:10.1029/2008JC004966, 2009

Click Here for Full Article

Heat flux across the surface of a macrotidal flat in southwest Korea

Tae-Wan Kim[1] and Yang-Ki Cho[1]

Received 16 June 2008; revised 25 March 2009; accepted 5 May 2009; published 30 July 2009.

[1] Temporal-spatial variations of heat fluxes between the tidal flat and seawater or atmosphere across the surface of a tidal flat were investigated from observed sediment, seawater, and atmosphere temperatures. The tidal flat receives heat from seawater during morning inundation, while heat exchange is reversed during afternoon inundation. Heat fluxes at tidal flat and seawater or atmosphere interface have a good relationship with exposure time in each station. Heat exchange between the tidal flat and seawater or atmosphere over the entire tidal flat was estimated from the correlation between heat flux and exposure time. In spring, summer, and autumn, the tidal flat gained mean heat of 2.352, 0.949, and 0.899 MJ m^{-2} from the atmosphere over each daytime exposure but lost 1.904, 0.955, and 1.680 MJ m^{-2} over each nighttime exposure, respectively. In spring, summer, and autumn, the tidal flat gained mean heat of 0.459, 0.336, and 0.601 MJ m^{-2} from seawater over each morning inundations and supplied mean heat of 0.530, 0.364, and 0.505 MJ m^{-2} to seawater over each afternoon inundation, respectively.

Citation: Kim, T.-W., and Y.-K. Cho (2009), Heat flux across the surface of a macrotidal flat in southwest Korea, *J. Geophys. Res.*, *114*, C07027, doi:10.1029/2008JC004966.

1. Introduction

[2] The heat flux across the surface of a tidal flat is a primary factor controlling biological and physical processes of the ecosystem and local climate in a coastal area. Water temperature in a shallow tidal flat region shows short-term variability due to heat exchange between seawater, the tidal flat and atmosphere [*Harrison and Phizacklea*, 1985]. Variation in seawater temperature can influence local ecosystems [*Tang et al.*, 2003] and weather [*Cho et al.*, 2000]. Accurate estimation of the heat exchange between the tidal flat, seawater and atmosphere is not only important for understanding local biological and physical systems, but essential in investigating macrotidal flat processes [*Guarini et al.*, 1997].

[3] A number of studies have looked into heat exchanges between a tidal flat, seawater and atmosphere [*Harrison and Phizacklea*, 1985; *Harrison*, 1985; *Vugts and Zimmerman*, 1985]. *Harrison* [1985] calculated heat exchange between a tidal flat and seawater from observations of mud temperature at four depths (25, 75, 200 and 280 mm). He found that the magnitude and direction of heat flux across the surface of a tidal flat are dependent on atmospheric and sea conditions, as well as on the timing of tidal inundation. The direction of heat flux between seawater and a tidal flat depends on their individual seasonal temperature differences, if heat convection is negligible in the tidal flat [*Harrison and Phizacklea*, 1985]. Tidal flats gain heat from seawater during winter, but lose heat to seawater during summer. *Vugts and Zimmerman* [1985] estimated the heat flow between seawater, a tidal flat and the atmosphere during inundation at Mok bay, western Dutch Wadden Sea, and suggested the possibility of predicting daily mean seawater temperature on the basis of the calculated heat exchange between these environments. The temperature of a tidal flat might differ spatially because of the heterogeneity in sediment properties (grain size, component and sedimentary structure) and water content. Also, the temperature of a tidal flat might change horizontally according to exposure time, as heat exchange between a tidal flat, seawater and atmosphere differs because of variable surface elevation. However, the majority of historical investigations did not consider spatial variation of heat flux, but used spatially limited data for calculating the heat flux. Previous measurements would therefore be insufficient for estimating the heat flux over an entire tidal flat with variable surface elevation.

[4] Spatial and temporal variations of temperature in a macrotidal flat were reported from intensive observation during our previous study [*Cho et al.*, 2005]. Variability in temperature of a tidal flat is closely related to the exposure time. This leads us to believe that heat flux between a tidal flat and seawater might be well related to the exposure time because the heat flux across the tidal flat surface depends on the temperature gradient. In this study, heat flux between a macrotidal flat and seawater or atmosphere during exposure and inundation periods was calculated from observed temperatures at five stations, with different exposure time for each season. The exchanged heat during exposure and inundation periods over entire tidal flat was quantitatively estimated using the relationship between heat flux and exposure time for each season.

2. Field Measurements

[5] The study site, the Baeksu macrotidal flat, which is approximately 8–10 km long and 4–6 km wide, is located

[1]Faculty of Earth System and Environmental Sciences, Chonnam National University, Kwangju, South Korea.

0148-0227/09/2008JC004966$09.00

along the southwestern coast of Korea (Figure 1). Local time (LT) (Korea Standard Time (KST)) uses Tokyo (135° in latitude), which precedes UTC (Universal Time Coordinated) by 9 h. The tide is principally semidiurnal, with mean spring and neap tidal ranges of 5.4 and 2.4 m, respectively. Most of the surface sediments were silt in the study area. Table 1 shows the surface sediment composition at each station observed by *Yang* [2000] in summer. The tidal flat, which is characterized by fine sediments and a gentle slope, was saturated by seawater during the exposure period.

[6] Sediment temperatures were measured every 3 min at six different levels (−2, −5, −10, −20, −30 and −40 cm), while water temperature was measured 5 cm above the tidal flat at five stations for 45 days during each season (Figure 2a). We define sediment temperature as the temperature of mixture of solid, pore water and air. The temperature measurements were made using Onset Computer Corporation HOBO temperature loggers, with a resolution of 0.02°C and accuracy of 0.2°C.

[7] Exposure time was calculated using sea level data estimated at each station. This estimate was acquired from relative variations between the standard tidal station (10 km to the north from station 1) and observation stations. To calculate relative differences between each station and the tidal station, sea level was measured at each station for 15 days. The solar radiation, wind velocity and direction, air temperature, air pressure and relative humidity were measured by an automated weather station (AWS) installed at a station near the coast (Figure 1). All data were averaged at 30 min intervals for analysis.

[8] The slopes between neighboring two stations were 0.13° (stations 1 and 2), 0.09° (stations 2 and 3), 0.06° (stations 3 and 4) and 0.04° (stations 4 and 5). The slope was decreasing to the offshore. Mean slope of the observation line from station 1 to 5 was approximately 0.09°. The

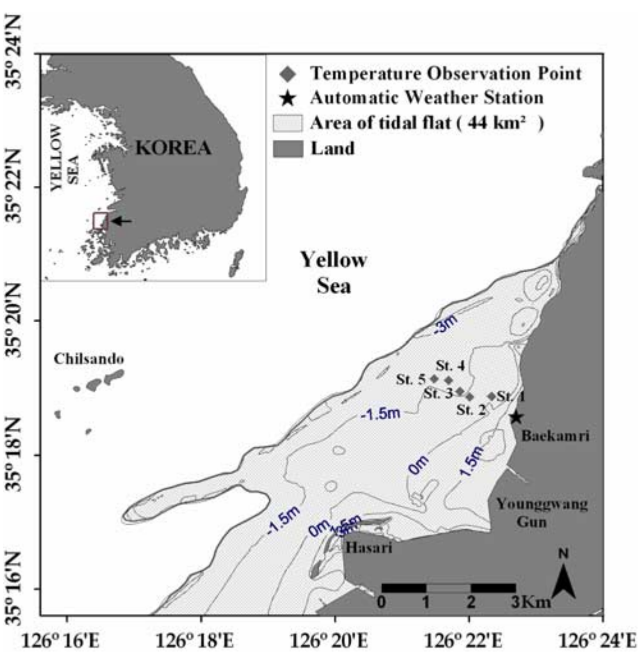

Figure 1. Map of the study area showing the observation stations on the Baeksu intertidal flat along western coast of Korea.

Table 1. Surface Sediment Composition for All Stations in Summer Season[a]

Station	Sand	Silt	Clay
1	6.57	67.26	26.17
2	37.90	50.99	11.11
3	33.57	53.67	12.76
4	15.02	65.92	19.07
5	12.12	78.45	9.43

[a] *Yang* [2000].

exposure-time ratio, calculated between relative exposure time and total observation time, was approximately 52% and 18% at stations 1 and 5, respectively (Table 2). The exposure-time ratio decreased with increasing distance offshore. Some data were poor because of erosion of the tidal flat. The observation depths of the sediment temperature were greatly changed because of erosion and deposition by strong winter storms.

[9] Near-surface sediment temperature is greatly influenced by atmospheric conditions and periods of exposure and inundation by tide. Figure 3 shows the time series variation of near-surface sediment and seawater temperature, tide and solar radiation at station 1 for each season. High tide was delayed by 48 min d^{-1} because of the dominant M_2 tide (12 h and 24 min period). Sediment temperature demonstrated a complex waveform since the frequencies and phase of solar radiation and tidal height are slightly different.

[10] Variation in sediment temperatures was similar to that of seawater temperature because of heat exchange between them during inundation periods across all seasons. In spring, maximum surface sediment temperatures during daytime exposure were more than 30°C, and decreasing during inundation because of heat loss to seawater. In summer, the highest sediment temperature of 36.4°C was recorded at 1200 LT on 15 August. The variation range in sediment temperatures was smaller during summer than spring. This was expected, as sediment temperatures are warmed up by higher air temperatures during nighttime exposure in summer.

[11] Surface sediment temperatures increased during morning inundation by relatively warm seawater in autumn. Temperatures increased slightly during daytime exposure because of the weak solar radiation. The range of sediment temperatures variation during winter was the smallest among the four seasons because of low-level solar radiation and short sunshine duration. During all seasons, the range of variation in sediment temperature decreased with depth.

3. Temporal Heat Flux Variation

[12] Tidal flats exchange heat with the atmosphere and seawater during exposure and inundation periods, respectively. If there is no heat source or sink in tidal flat, the surface heat flux is equal to the sum of the heat content change in tidal flat and the conductive heat flow at the lowest measured depth [*Kim et al.*, 2007]. Surface erosion and deposition often change sediment thickness, which in turn influences observation depth of the temperature logger. The temperature at a depth of 0.01 m was calculated as a reference value at each station in order for the exact heat

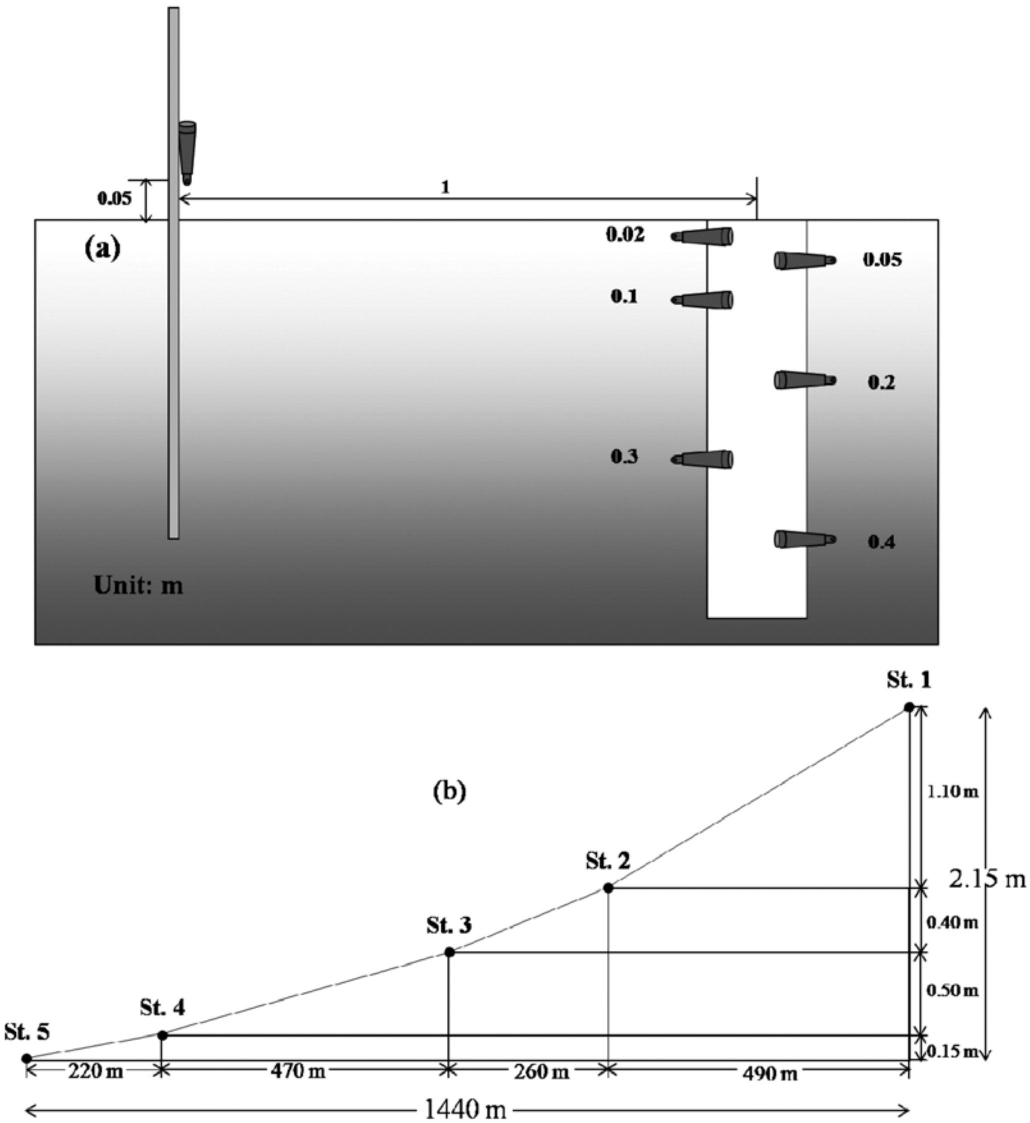

Figure 2. (a) Schematic figure of the sediment temperature observation at each station. (b) Distance and vertical height between stations along the observation line.

exchange between tidal flat, atmosphere and seawater to be calculated.

[13] During exposure periods, the net heat exchange between tidal flat and atmosphere may be expressed as

$$Q_{Mud\text{-}Air} = Q_s - (Q_l + Q_e + Q_h), \tag{1}$$

where $Q_{Mud\text{-}Air}$ is the net heat exchange between tidal flat and atmosphere, and Q_s is the incoming short-wave solar radiation. Q_l, Q_e and Q_h are the long-wave radiation, latent heat transfer and sensible heat flux from the tidal flat surface to atmosphere, respectively. Details of each term are explained in Appendix A.

[14] During inundation, net heat flux between the tidal flat and seawater is given by the equation of *Losordo and Piedrahita* [1991]:

$$Q_{Mud\text{-}Sea} = C_s \frac{\kappa}{H_{Sed}/2}(T_S - T_M), \tag{2}$$

where H_{Sed} is the effective thickness of the sediment layer (m), T_S is the seawater temperature at the tidal flat seawater interface, T_M is the calculated 0.01 m sediment temperature and C_s and κ are the volumetric heat capacity (3.65×10^6 J m^{-3} K^{-1}) and thermal diffusivity ($0.38-0.64 \times 10^{-6}$ m^2 s^{-1}) of the sediment, respectively [*Kim et al.*, 2007].

[15] Figure 4 shows the time series variations in solar radiation, heat flux across the tidal flat surface and sea level at station 1 during spring. A positive heat flux represents heat gain in the tidal flat. The variation of solar radiation is

Table 2. Exposure-Time Ratio for Each Station[a]

Station	Exposure-Time Ratio (%)
1	52.1
2	33.9
3	29.2
4	22.5
5	17.9

[a]Time ratio between relative exposure-time and total observation time.

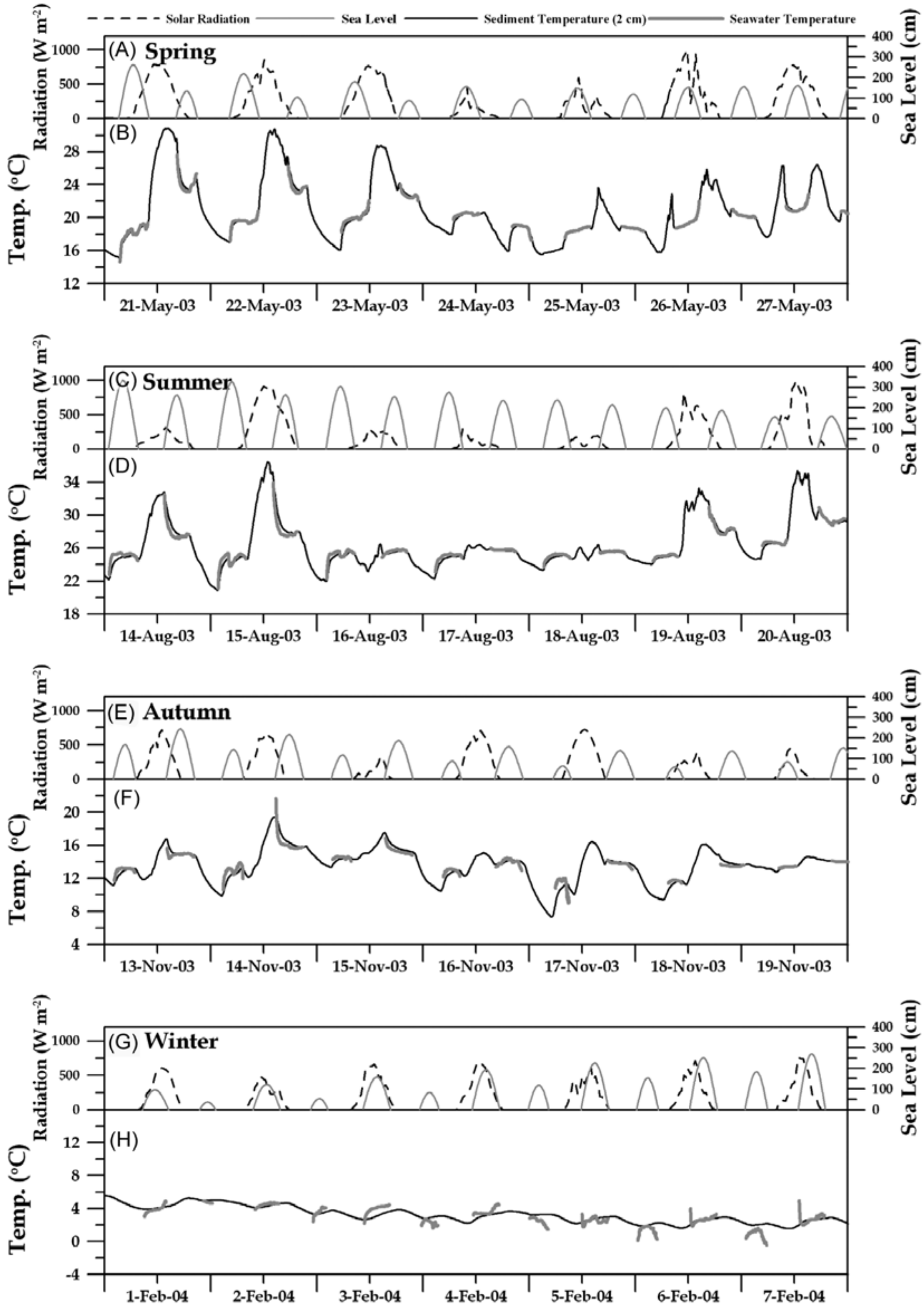

Figure 3. Time series variations at station 1 for 7 days during (a and b) spring, (c and d) summer, (e and f) autumn, and (g and h) winter in seawater 5 cm above the tidal flat and sediment temperatures 2 cm within tidal flat (Figures 3b, 3d, 3f, and 3h), sea level (solid line in Figures 3a, 3c, 3e, and 3g), and solar radiation (dotted line in Figures 3a, 3c, 3e, and 3g).

an important factor in the variability of heat flux between atmosphere and tidal flat during daytime exposure. The heat flux was approximately 400 W m^{-2} during daytime exposure on 21 May 2003, with solar radiation of about 800 W m^{-2}. The tidal flat supplied about 100 W m^{-2} to the atmosphere during nighttime exposure as a result of relatively colder air on 21 May 2003.

[16] Heat flux across the surface of a tidal flat during inundation depends on temperature differences between the tidal flat and seawater. A tidal flat heated by strong solar

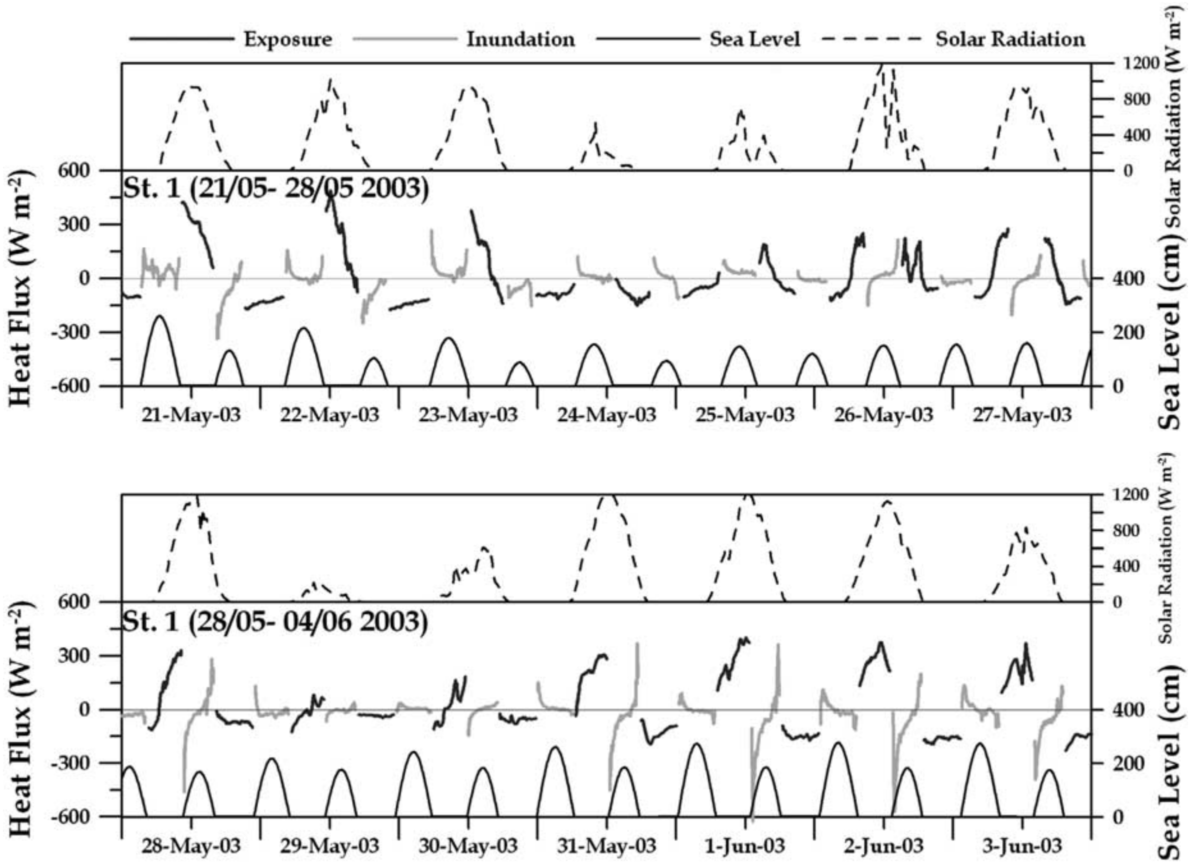

Figure 4. Time series variations in the solar radiation, sea level, and heat flux between the tidal flat and atmosphere or seawater at station 1 from 21 May to 4 June 2003.

radiation during daytime exposure provides heat to the relatively cold seawater during the following flood tide. Seawater in shallower zones is heated more because of combined effects of solar radiation and the previously warmed tidal flat. The relatively warm seawater in the landward edge of the tidal flat provides partial heat to the tidal flat during ebb tides. During daytime exposure, the tidal flat was heated by the atmosphere, which in turn supplied heat to seawater during afternoon inundation. Conversely, the cooled tidal flat due to the heat exchange with the atmosphere during nighttime exposure gained heat from warm seawater during the following morning flood tide. The amount of heat exchange between the tidal flat and atmosphere or seawater may be influenced by high and low water time.

[17] Figure 5 shows the relationship between heat exchange and time of low and high water at tidal flat and atmosphere or seawater interface during each exposure and inundation period for each season. The *y* axis represents total heat exchange over each exposure (rectangular) and inundation (filled circle), while the *x* axis represents low and high tide times. Two solid curves are polynomial regression lines of heat exchange during exposure and inundation. The tidal flat gained a maximum of approximately 6.14 MJ m^{-2} heat from the atmosphere during exposure when low tide occurred at around 1200 LT at station 1 in spring. In return, the tidal flat provided a maximum of approximately 3.90 MJ m^{-2} heat to the atmosphere during exposure when low tide occurred at around 2300 LT at station 1 in spring.

[18] The tidal flat gained a maximum of 1.28 MJ m^{-2} heat from seawater at approximately 0900 LT and lost a maximum 1.62 MJ m^{-2} heat to seawater at approximately 1600 LT at station 1 in spring. The heat gained from seawater during morning (0000–1200 LT) at stations 2 (maximum: 1.75 MJ m^{-2}) and 3 (maximum: 1.98 MJ m^{-2}) was larger than that at station 1 because of the relatively long inundation period in spring. Heat exchanges between tidal flat and seawater at stations 4 and 5 were small because of short exposure time in spring. The range of heat exchange decreases to the offshore. It is noticeable that the amount of heat exchange is affected by the exposure-time ratio. The range of heat exchange between atmosphere and tidal flat during summer was smaller than that during spring because of weak solar radiation at station 1. During autumn, the magnitude of maximum heat exchange between atmosphere and tidal flat was comparable to that of summer at midday but the magnitude of minimum heat exchange was two times that of summer at midnight. The magnitude of heat exchange between atmosphere and tidal flat during winter was comparable to that of autumn at night. However, daytime heat exchange between atmosphere and tidal flat during winter was larger than during autumn.

[19] The tidal flat cooled during nighttime exposure after gaining heat from seawater during morning inundation. Conversely, it was heated during daytime exposure, after which it provided heat to seawater during afternoon inundation. The exchanged heat during exposure was 3–4 times larger than that during inundation. There was approximately

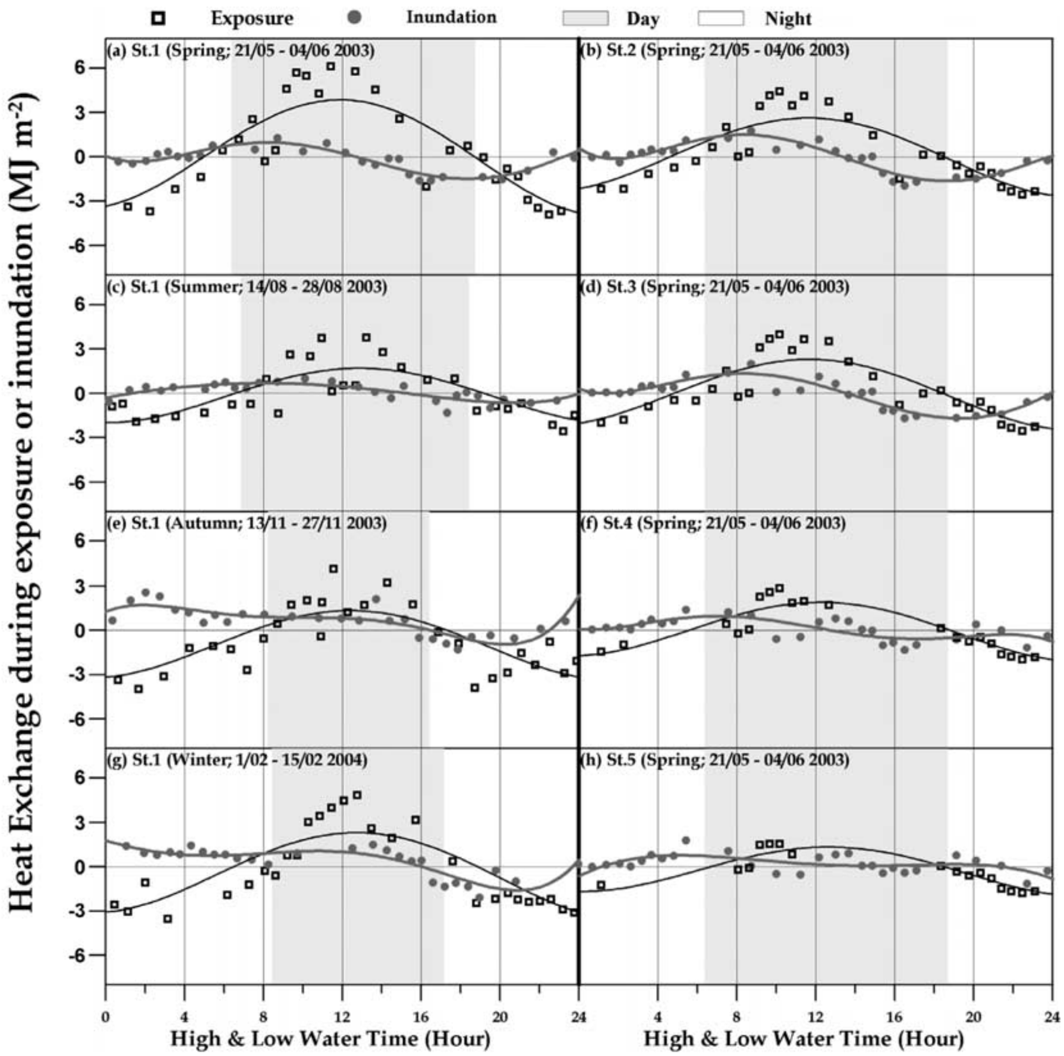

Figure 5. Relationship between the heat exchange at tidal flat and atmosphere interface during exposure (rectangle) or tidal flat and seawater interface during inundation (filled circle) and the time of low and high water for each season. Solid curves are polynomial regression lines of heat exchange during exposure and inundation.

a 6 h phase lag between the two heat exchanges. The magnitude of heat flux across the tidal flat surface during inundation might depend on the heat flux during the previous exposure period. Figure 6 shows the relationship between the heat fluxes during exposure and following inundation, depicting a good correlation at most stations, the exception being station 5 during spring. Slope of the fitted linear regression line varied from a minimum of -0.501 to a maximum of -0.237. The slope decreased at offshore stations with decreasing exposure-time ratio of the tidal flat. The slope of the fitted line also showed seasonal variation (minimum -0.421 to maximum -0.237) at station 1 due to different seawater temperatures.

4. Horizontal Structure of Heat Flux Over Tidal Flat and Its Temporal Variation

[20] Total heat exchange over the entire tidal flat can be estimated if the relationship between heat fluxes and exposure-time ratio at temperature observation stations is known. Heat exchange between the tidal flat, atmosphere and seawater changed in accordance with exposure-time ratio. The heat exchange during exposure can be assumed to be zero at the sublittoral zone, where the exposure-time ratio was zero. Similarly, the heat exchange during inundation was assumed to be zero at the supralittoral zone, which was always exposed. The relationship between heat flux across the tidal flat surface and exposure-time ratio during exposure and inundation was calculated using a polynomial fitting equation for each season (Figure 7). Positive and negative heat fluxes occur during daytime and nighttime exposures and morning and afternoon inundations, respectively. Four relationships were calculated between the heat flux and exposure-time ratio according to heat gained and lost during exposure and inundation periods, respectively. The lines fitted during exposure show a linear relationship between heat flux and exposure-time ratio. Heat flux across the tidal flat surface during exposure was zero at the sublittoral zone, but gradually increased with exposure-time ratio, regardless of season. However, the lines fitted during

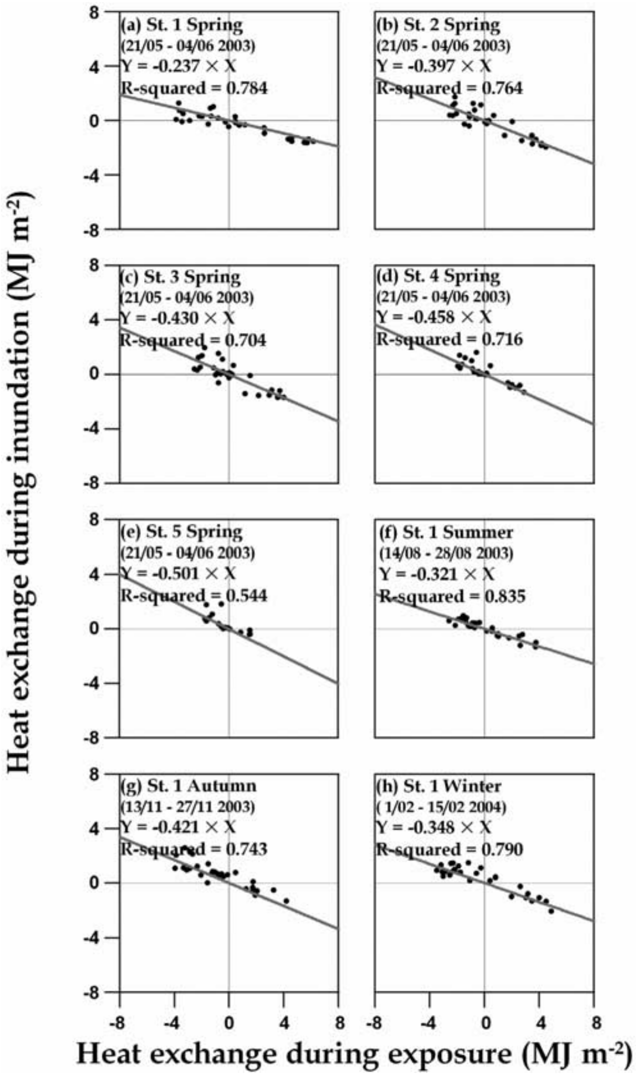

Figure 6. The relationship between heat fluxes at tidal flat surface during exposure and the following inundation. Solid lines are linear regression lines of heat exchange during exposure and inundation.

morning and afternoon inundations were convex and concave, respectively.

[21] The amount of heat exchange at station 1, where exposure-time ratio was the longest of all observation stations, was the largest during daytime exposure and smallest during nighttime exposure during each season (Figure 7). Conversely, the amount of heat exchange at station 5 was the smallest of all observation stations. Heat gained from the atmosphere during daytime exposure at station 1 was largest during spring. In summer, total irradiance for observation periods was less than that of spring. Also, heat released by tidal flat to the atmosphere during nighttime exposure was smaller during summer than both spring and autumn. This was attributed to insufficient heating of the tidal flat during daytime exposure. Heat flux at the tidal flat and atmosphere interface was positive during daytime exposure and negative during nighttime exposure, regardless of season, with similar magnitudes for each season.

[22] The magnitudes of heat exchange at stations 2 and 3 during inundation were larger than both offshore and onshore stations. Although the amount of heat exchange during exposure was largest at station 1, the heat exchange between tidal flat and seawater was small because of relatively short inundation time. The exchanged heat during inundation at stations 4 and 5 was relatively small, which was attributed to short exposure time. Seasonal heat exchange over the entire tidal flat was estimated using the relationship between heat flux and exposure-time ratio. Heat exchange during winter could not be estimated because of failure in collecting available data as a result of erosion by wind storms.

[23] Figure 8 shows the horizontal distributions of exposure-time ratios and heat exchange during daytime and nighttime exposures and morning and afternoon inundations over the entire tidal flat during spring. The average exposure-time ratio over the entire tidal flat was approximately 40.6%. The tidal flat gained a mean 2.352 MJ m^{-2}

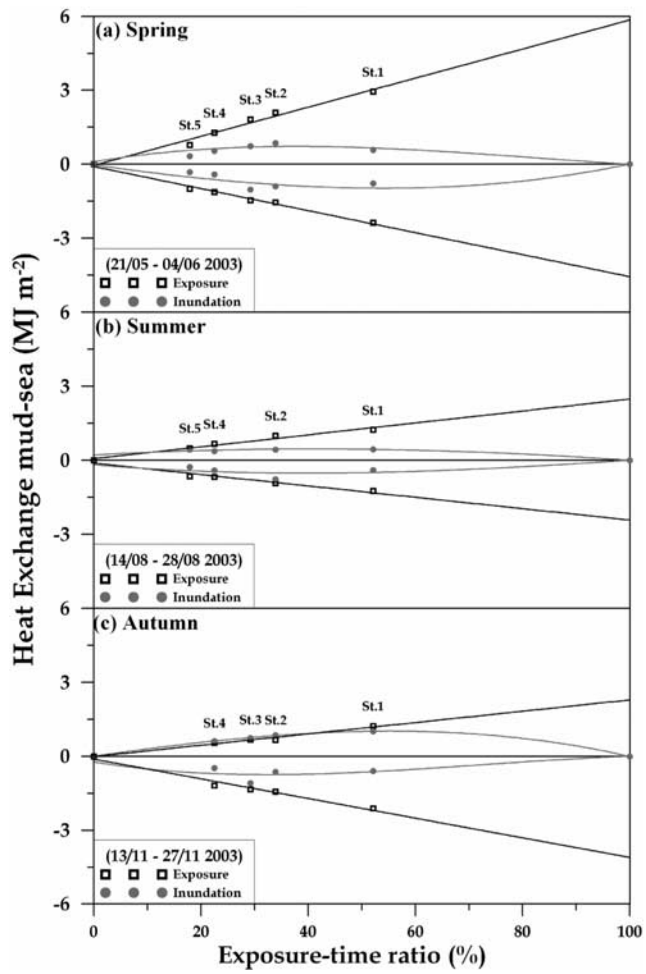

Figure 7. Seasonal variation in the relationship between the heat exchange and exposure-time ratio during exposure and inundation. Positive heat flux occurs during daytime exposure and morning inundation. Negative heat flux occurs during nighttime exposure and afternoon inundation. Solid lines are linear (during exposure) and polynomial regression (during inundation) lines between exposure-time ratio and heat exchange.

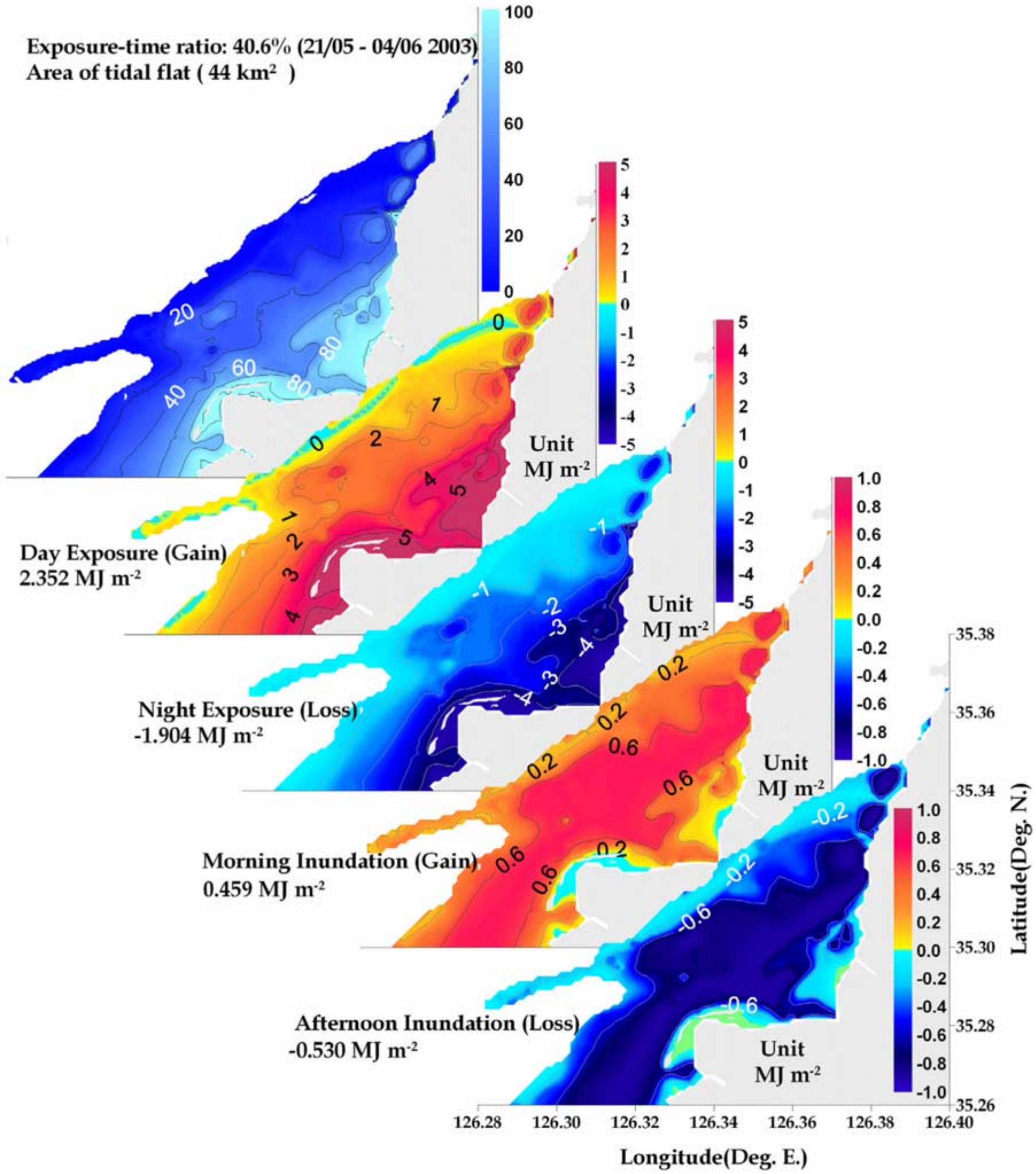

Figure 8. Horizontal distribution of exposure-time ratio (first panel) and amount of heat exchange between the tidal flat and atmosphere (second and third panels) or seawater (fourth and fifth panels) during spring 2003.

of heat from the atmosphere over each daytime exposure period, and supplied a mean 1.904 MJ m^{-2} of heat to the atmosphere over each nighttime exposure period. The tidal flat gained a mean 0.459 MJ m^{-2} of heat from seawater over each morning inundation period, and supplied a mean 0.530 MJ m^{-2} of heat to seawater over each afternoon inundation period. In spring, the tidal flat was heated by the atmosphere during exposure and supplied heat to seawater during inundation.

[24] The amount of heat exchange during daytime exposure was smaller in summer than in spring, attributed to less solar radiation during observation periods (Figure 9). Average exposure time ratio was approximately 36.5% in summer. The tidal flat gained a mean 0.949 MJ m^{-2} of heat from the atmosphere over each daytime exposure period and supplied a mean 0.955 MJ m^{-2} of heat to the atmospheric over each nighttime exposure period. The tidal flat gained a mean 0.336 MJ m^{-2} of heat from seawater over each morning inundation and supplied a mean 0.364 MJ m^{-2} of heat to seawater over each afternoon inundation period. Magnitudes of net heat flux at tidal flat and atmosphere or seawater interface during exposure or inundation were almost zero in summer.

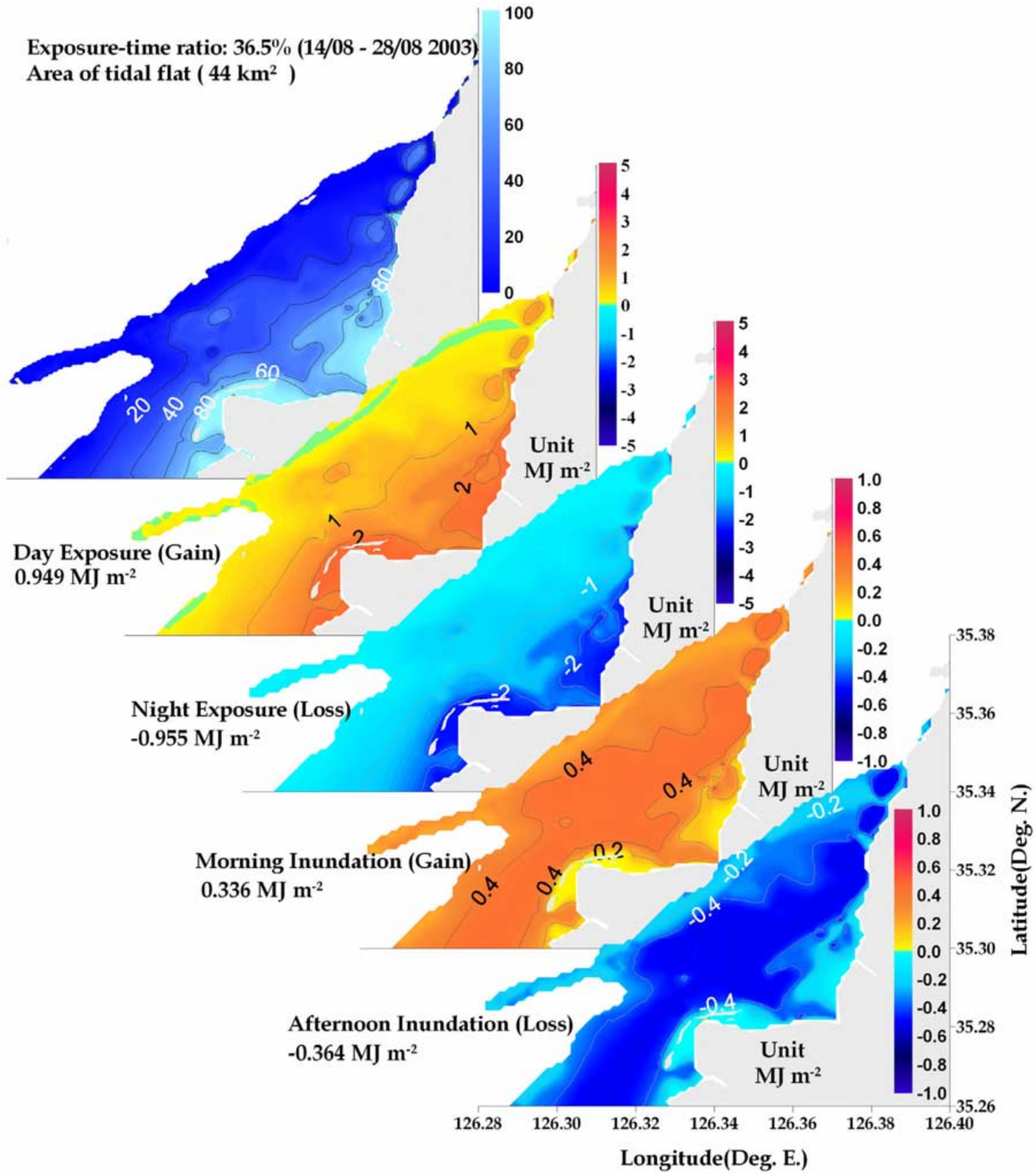

Figure 9. Horizontal distribution of exposure-time ratio (first panel) and amount of heat exchange between the tidal flat and atmosphere (second and third panels) or seawater (fourth and fifth panels) during summer 2003.

[25] Exchanged heat during daytime exposure was smallest in autumn because of lower levels of solar radiation and short daylight period (Figure 10). The average exposure-time ratio was approximately 39.4%. The tidal flat gained a mean 0.899 MJ m^{-2} of heat from the atmosphere over each daytime exposure period and supplied a mean 1.680 MJ m^{-2} of heat to the atmosphere over each nighttime exposure period in autumn. The tidal flat gained a mean 0.601 MJ m^{-2} of heat from seawater over each morning inundation period and supplied a mean 0.505 MJ m^{-2} of heat to seawater over each afternoon inundation period. The tidal flat was cooled by the atmosphere during nighttime exposure and gained heat from the seawater during inundation the following morning.

5. Conclusions

[26] Heat exchange between a macrotidal flat and seawater or atmosphere was estimated on the basis of intensive temperature observations. Heat flux across the tidal flat surface is affected by solar radiation and tidal period. The tidal flat provides heat to seawater during afternoon inundation, and receives heat from seawater during morning inundation. The heat flux has a good relationship with exposure-time ratio for each season. The amount of heat

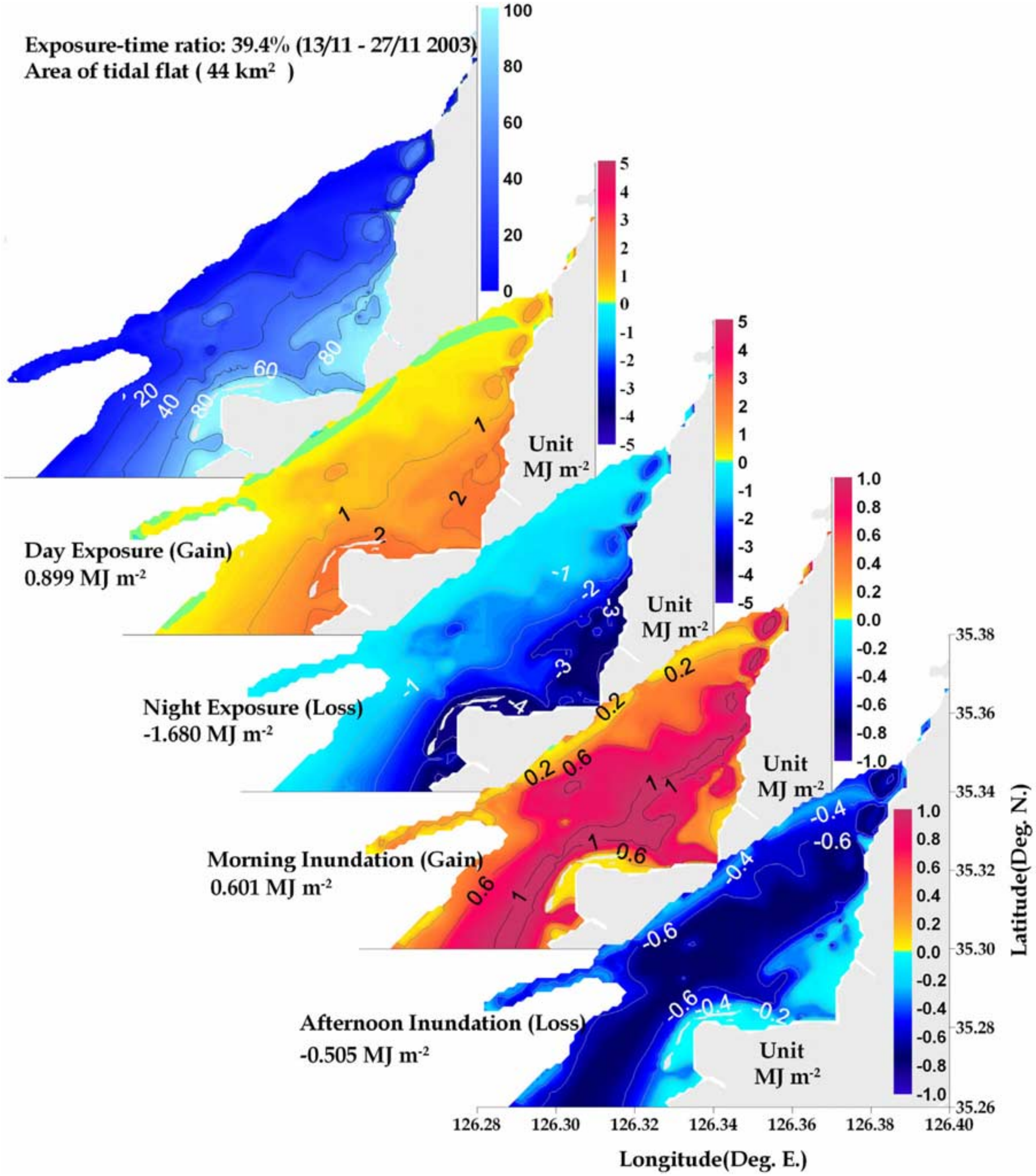

Figure 10. Horizontal distribution of exposure-time ratio (first panel) and amount of heat exchange between the tidal flat and atmosphere (second and third panels) or seawater (fourth and fifth panels) during autumn 2003.

exchange between the tidal flat and seawater during inundation depends on heat exchange between the tidal flat and the atmosphere during previous exposure. Slope of the fitted linear regression line between the heat flux at tidal flat surface during exposure and following inundation varied from -0.501 to -0.237 according to the exposure-time ratio and seawater temperature.

[27] Total exchanged heat between tidal flat and seawater or atmosphere over the entire tidal flat was calculated using the correlation between heat flux and exposure-time ratio in each season. The tidal flat heat gain means were 2.352, 0.949 and 0.899 MJ m^{-2} from the atmosphere over each daytime exposure period for spring, summer and autumn of 2003, respectively, while heat loss means were 1.904, 0.955 and 1.680 MJ m^{-2} to the atmosphere over each nighttime exposure period. Also, tidal flat heat gain means were 0.459, 0.336 and 0.601 MJ m^{-2} from seawater over each morning inundation period for spring, summer and autumn of 2003, respectively, while heat loss means were 0.530, 0.364 and 0.505 MJ m^{-2} to seawater over each afternoon inundation period.

[28] The results of this study are important as they will enable us to predict short-term variation in water temperature and local climate in coastal areas with a macrotidal flat.

Appendix A

[29] The heat flux on tidal flat surface was calculated using the estimated 0.01 m sediment temperature through the following equation:

$$\frac{T_i^{n+1} - T_i^n}{\Delta t} = \kappa \frac{T_{i+1}^n - 2T_i^n + T_M^n}{(\Delta z)^2}, \tag{A1}$$

where Δt is the time interval (180 s), T_M^n is the sediment temperature of 0.01 m depth at *nth* time (°C), T_i is observed sediment temperature at *i*th layer (°C) and Δz is the depth thickness of the each layer (m)and κ is the thermal diffusivity at *i*th layer ($m^2\ s^{-1}$). The sediment temperature at 0.01 m depth T_M^n can be obtained by the following equation:

$$T_M^n = 2T_i^n - T_{i+1}^n + \left(\frac{(\Delta z)^2}{\kappa}\right)\left(\frac{T_i^{n+1} - T_i^n}{\Delta t}\right). \tag{A2}$$

The net incoming solar radiation on the tidal flat surface is represented as

$$Q_s = (1 - \alpha)\, Q_{s0}, \tag{A3}$$

where Q_{s0} is measured by solar radiation at the automatic weather station ($W\ m^{-2}$) and α is albedo on the tidal flat surface (0.17).

[30] The long-wave heat flux is given by [*May*, 1986]

$$Q_l = \left\lfloor \varepsilon\sigma T_a^4 \left(0.4 - 0.05 e_a^{1/2}\right) + 4\varepsilon\sigma T_a^3 (T_M - T_a) \right\rfloor \times \left(1 - 0.75 C^{3.4}\right), \tag{A4}$$

where ε is emissivity of the tidal flat (0.96 [*van Bavel and Hillel*, 1976]), σ is Stefan-Boltzman constant (5.6705 × $10^{-8}\ W\ m^{-2}\ K^{-4}$), T_M is the absolute temperature (i.e., K) of the tidal flat surface, T_a is the absolute air temperature above the tidal flat, e_a is vapor pressure of the air above the tidal flat (*kPa*) and C is the amount of cloud in tenths.

[31] The sensible heat transfer on a tidal flat surface is given by [*Businger*, 1973; *Stathers et al.*, 1988; *Guarini et al.*, 1997]:

$$Q_h = \rho_a C_{Pa} C_h (1 + U)(T_M - T_a), \tag{A5}$$

where ρ_a is density of air (1.2929 kg m^{-3}), C_{Pa} is specific heat of air at constant pressure (1003.0 J kg^{-1} K^{-1}), C_h is bulk transfer coefficient for conduction (0.0014) and U is wind speed (m s^{-1}).

[32] The latent heat transfer on the tidal flat surface is given by [*Guarini et al.*, 1997]

$$\begin{aligned} Q_e &= \xi V_W \\ V_W &= \rho_a L_V C_V (1 + U)(q_M - q_a) \\ L_V &= (2500.84 - 2.35(T_M - 273.16)) \times 10^3 \\ q_M &= \frac{0.621 P_{sat}^{\vee}}{P_{Atm} - (1 - 0.621) P_{sat}^{\vee}}, \end{aligned} \tag{A6}$$

where ξ is the water content of the tidal flat surface, L_V is the latent heat of evaporation (J kg^{-1}), C_V is the bulk transfer coefficient for conduction (0.0014), U is the wind speed (m s^{-1}), q_M is the specific humidity of saturated air at water temperature, q_a is the specific humidity of air, $P_{sat}^{\vee}$ is the vapor pressure (*kPa*) in saturation at interstitial water temperature [*Goff*, 1957], and P_{Atm} is atmosphere pressure.

[33] **Acknowledgment.** This work was funded by the Korea Meteorological Administration Research and Development Program under grant CATER 2009-4506.

References

Businger, J. A. (1973), Turbulent transfer in the atmospheric surface layer, in *Workshop on Micrometeorology*, edited by D. A. Haugen, pp. 67–100, Am. Meteorol. Soc., Boston, Mass.
Cho, Y. K., M. O. Kim, and B. C. Kim (2000), Sea Fog around the Korea Peninsula, *J. Appl. Meteorol.*, *39*, 2473–2479.
Cho, Y. K., T. W. Kim, K. W. You, L. H. Park, H. T. Moon, S. H. Lee, and Y. H. Youn (2005), Temporal and spatial variabilities in the sediment temperature on the Baeksu tidal flat, Korea, *Estuarine Coastal Shelf Sci.*, *65*, 302–308, doi:10.1016/j.ecss.2005.06.010.
Goff, J. A. (1957), Saturation pressure of water on the new Kelvin temperature scale, *ASHRAE Trans.*, *63*, 347–354.
Guarini, J. M., G. F. Blanchard, P. Gros, and S. J. Harrison (1997), Modeling the mud surface temperature on intertidal flats to investigate the spatio-temporal dynamics of the benthic microalgal photosynthetic capacity, *Mar. Ecol. Prog. Ser.*, *153*, 25–36, doi:10.3354/meps153025.
Harrison, S. J. (1985), Heat exchange in muddy intertidal sediments, Chichester Harbour, West Sussex, England, *Estuarine Coastal Shelf Sci.*, *20*, 477–490, doi:10.1016/0272-7714(85)90090-3.
Harrison, S. J., and A. P. Phizacklea (1985), Seasonal changes in heat flux and heat storage in the intertidal mudflats of the Forth estuary, Scotland, *Int. J. Climatol.*, *5*, 473–485, doi:10.1002/joc.3370050502.
Kim, T.-W., Y.-K. Cho, and E. P. Dever (2007), An evaluation of the thermal properties and albedo of a macrotidal flat, *J. Geophys. Res.*, *112*, C12009, doi:10.1029/2006JC004015.
Losordo, T. M., and R. H. Piedrahita (1991), Modeling temperature variation and thermal stratification in shallow aquaculture ponds, *Ecol. Modell.*, *54*, 189–226, doi:10.1016/0304-3800(91)90076-D.
May, P. W. (1986), A brief explanation of Mediterranean heat and momentum flux calculations, NORDA Code 322, Nav. Ocean Res. and Dev. Activity, NSTL Station, Miss.
Stathers, R. J., T. A. Black, W. G. Bailey, and M. D. Novak (1988), Modeling surface energy fluxes and temperature in dry and wet bare soils, *Atmos. Ocean*, *26*, 59–73.
Tang, D. L., H. Kawamura, M. A. Lee, and T. V. Dien (2003), Seasonal and spatial distribution of chlorophyll-a concentrations and water conditions in the Gulf of Tonkin, South China Sea, *Remote Sens. Environ.*, *85*, 475–483, doi:10.1016/S0034-4257(03)00049-X.
van Bavel, C. H. M., and D. I. Hillel (1976), Calculating potential and actual evaporation from a bare soil surface by simulation of concurrent flow of water and heat, *Agric. Meteorol.*, *17*, 453–476, doi:10.1016/0002-1571(76)90022-4.
Vugts, H. F., and J. T. F. Zimmerman (1985), Heat balance of a tidal flat area, *Neth. J. Sea Res.*, *19*, 1–14, doi:10.1016/0077-7579(85)90037-7.
Yang, B. C. (2000), Seasonal cycle of surface sediment distribution and evolution of sedimentary facies on the Baeksu intertidal flat, south western coast of Korea Peninsula, MSc. thesis, 147 pp., Chonnam Natl. Univ., Kwangju, South Korea.

Y.-K. Cho and T.-W. Kim, Faculty of Earth System and Environmental Sciences, Chonnam National University, 300 Yongbong-dong, Kwangju, 500-757 South Korea. (ykcho@chonnam.ac.kr)